Hindawi
International Journal of Intelligent Systems
Volume 2023, Article ID 6957327, 18 pages
https://doi.org/10.1155/2023/6957327

Research Article

Design of Adaptive Periodic Event-Triggered Mechanism-Based EID with MRC Based on PSO Algorithm for T-S Fuzzy Systems

Mohamed Soliman,[1] **Muhammad Majid Gulzar**,[1,2] **and Adnan Shakoor**[1,3]

[1]*Department of Control & Instrumentation Engineering, King Fahd University of Petroleum and Minerals, Dhahran 31261, Saudi Arabia*
[2]*Interdisciplinary Research Center for Renewable Energy and Power Systems (IRC-REPS), King Fahd University of Petroleum and Minerals, Dhahran 31261, Saudi Arabia*
[3]*Interdisciplinary Research Center for Health and Life Sciences & Engineering, King Fahd University of Petroleum & Minerals, Dhahran 31261, Saudi Arabia*

Correspondence should be addressed to Adnan Shakoor; adnan.shakoor@kfupm.edu.sa

Received 29 May 2023; Revised 4 September 2023; Accepted 2 November 2023; Published 27 November 2023

Academic Editor: Surya Prakash

This article discusses issues with disturbance rejection and periodic signal tracking in a specific type of time-varying delay nonlinear systems. The proposed approach, known as the modified repetitive controller (MRC) scheme, utilizes an equivalent-input-disturbance (EID) estimator to enhance the system's performance. It effectively improves the system's ability to reject both aperiodic and periodic unknown disturbances, while also achieving accurate tracking of periodic reference signals. A T-S fuzzy model has been used to roughly represent the system nonlinearity. Additionally, a fuzzy state observer based on an adaptive periodic event-triggered mechanism (APETM-FSO) has been used to decrease data transfer, energy use, and communication resource utilization. The APETM is able to identify the occurrence of an event by surpassing a predetermined threshold with the error signal, thanks to the designed adaptive event triggering condition. Transmission of the current data only takes place when the event happens, while data can remain unchanged using a zero-order hold if the event does not occur. In addition to, controller parameters are tuned using a particle swarm optimization (PSO) approach. Hence, T-S fuzzy model-based EID, MRC, FSO-APETM, and PSO construct the overall system. In order to ensure the asymptotic stability of the entire system in the presence of unknown disturbances, the article establishes sufficient conditions using the Lyapunov–Krasovskii functional stability theory and linear matrix inequalities (LMIs). These conditions are derived to guarantee the desired stability properties of the system. To demonstrate the effectiveness and feasibility of the proposed scheme, simulation results with comparative study are presented. The proposed controller has achieved better tracking performance with less tracking error with maximum value of 0.05. In addition, the suggested APETM has minimum triggering times which is 34 as comparison with PETM which is 40 times, and hence, APETM is more effective than PETM in reducing data transmission frequency and using less communication resources overall.

1. Introduction

In control systems, there are two main important issues, the periodic signal tracking and the rejection of unknown disturbances. One of the better control systems for tracking external periodic signals and adjusting the unknown periodic disturbances through repeated learning tasks is the repetitive control (RC) strategy [1]. The RC is widely used in many applications because it can produce a better control performance, including robotic manipulators, servo motors, power systems, inverted pendulums, and any systems that need to reject or follow periodic signals [2–4]. The RC control technique involves learning from past errors and modifying feedback control behavior for the following cycle. As a result, it is possible to decrease tracking error and track the reference input with output that is steady-state error-free. A low-pass filter (LPF) has been added to the RC scheme to create the modified RC (MRC) scheme in order to

stabilize precisely appropriate plants, which are more challenging for the RC method [5]. The incorporated LPF can reject the high-frequency signals besides, improving the stability and significantly decreasing the control effort. The incorporation of this approach guarantees that the steady-state tracking error in MRC systems is reduced compared to that of RC systems, resulting in an enhanced tracking performance [5]. The effects of aperiodic disturbances cannot be rejected with MRC scheme as well as the periodic ones because the RC feedback loop is unable to achieve it [6], and this is a drawback for MRC scheme. Usually in practice, disturbances commonly combine periodic and aperiodic elements, and they happen at a range of frequencies. Therefore, a number of control methods have been developed in order to overcome these disturbances [7–10] and the references therein. It has been determined how much of an impact output disturbances have using the disturbance observer [8]. However, it is quite challenging to design the filter for the disturbance observer because of the stability of the overall system. In [8], high order RC technique, which has been described as robust, handled the both components of disturbances. Although an ideal performance balance has been reached for the disturbances, one of the two types of control performance has been degraded. The MRC scheme has been enhanced by integrating an equivalent-input-disturbance (EID) estimator, which serves as a developed approach to compensate for both aperiodic and periodic disturbances. This integration ensures that the MRC is capable of effectively mitigating the impact of both types of disturbances [9]. It is simple to implement EID into practice due to its resilience in mitigating the disruptions. In addition, various control systems have been presented EID-based control techniques, such as [11, 12], due to its efficient performance.

On the other hand, in most of the practical applications, the nonlinearity has been appeared such as in power systems, robots, and numerous physical systems [5, 13–16]. Therefore, a variety of control mechanisms have been developed to handle these nonlinear systems. The T-S fuzzy model is one of the methods used in system modeling and control, and it can effectively characterize nonlinear systems and well approximate the nonlinearity with the aid of the universal approximation technique [16–18]. In comparison to other fuzzy models, the T-S fuzzy model can more accurately mimic nonlinearity in real systems for the same nonlinear systems with fewer rules. More recent works for T-S fuzzy systems have been presented [14–18]. For many nonlinear systems, MRC had been combined with the T-S fuzzy model such as [17, 18] to give an effective algorithm.

In addition to, the majority of systems heavily relied on continuous parameters to perform various tasks related to system modeling and control. Regardless of it is needed to update the data or not, the timing-triggered control updates it periodically. This may cause heavy communication load on the controller and sensors. Hence, much literature introduced the event-triggered mechanism (ETM) [15, 19–21]. The ETM has a control flexibility and can save more communication resources compared to the other schemes. According to the designed ET condition, ETM can detect the occurrence of an event. This mechanism is incorporated to decide that it is needed to send a new data or not according to ET condition through communication channels. This designed condition depends on an error signal in which it goes over a set limit. The data will not be sent until the condition is achieved, and it will be maintained and preserved using a zero-order hold (ZOH) technique, which involved holding their values constant until the next update or sampling point. Unfortunately, because of continuous sampling which is dependent on the frequency of the conditions achieving, the majority of ETM techniques result in undesirable Zeno behavior [19]. A solution to this issue has been proposed in [19, 20] by the creation of a periodic ETM (PETM), which periodically assesses an ET condition at a predetermined sample time to decide whether or not to broadcast a new control signal.

Additionally, a static triggering condition was considered when designing the PETM, which could be troublesome if the dynamics of the system alter due to the static triggering condition's inability to change. An adaptive ETM (AETM) technique with an adaptive threshold has been studied in some studies to conserve more computing resources and react to changes in system dynamics [22, 23].

Additionally, five control schemes has been chosen and presented through this paper to enhance the MRC systems' control efficiency. Due to its efficiency and accuracy in approximation, some of these schemes adopted the T-S fuzzy model approach to approximate and characterize this nonlinearity. The first method [5] was developed for a family of nonlinear time delay systems. The purpose of a novel output feedback control methodology-based MRC scheme is to track a periodic reference signal through time but only with the exclusion of periodic disturbances. By using free-weighting matrix technique with Lyapunov–Krasovskii functional (LKF)-based fuzzy, the robust stability of the augmented system is guaranteed based on sum of sufficient conditions introduced in terms of LMIs. Two applied applications are subjected to demonstrate the theoretical findings of the suggested controller with better performance as compared with other existing schemes. However, this scheme cannot deal with the aperiodic disturbances.

The second scheme [17] is designed for the periodic tracking of nonlinear physical plant. The states of the majority of physically nonlinear systems are not quantifiable, as is well known. The sState observer is a filter used to get the states' information if the system is deterministic [24]. A novel fuzzy state observer (FSO) and fuzzy-based MRC have therefore been used as mixed controller for states estimating and periodic tracking. For the stability requirement of the entire closed-loop system, a fuzzy Lyapunov function is proposed in forms of LMIs. Separate designs for the MRC fuzzy controller and observer greatly increase designing freedom while requiring the least amount of computing. The efficacy and adaptability of the controller scheme have been verified by the outcomes of the simulation. However, also this scheme can deal only with the periodic disturbance type because there is not an estimator or any other technique for the aperiodic disturbances' rejection.

The third scheme one of these control schemes has been designed for a class of nonlinear systems with unknown external disturbance, which is an EID estimator-based MRC scheme [25]. This control scheme has been introduced in such improving the performance of disturbance rejection in the MRC system. Aperiodic disturbances' effects on the input are estimated and rejected. This has been achieved by incorporating the estimation mechanism into MRC law. The stability guarantee in this paper has been derived using the linear matrix inequality (LMI)-based Lyapunov function method. There are two tuning parameters which would be adjusted in order to achieving robust stability and improving the performances of both steady-state and transient behaviors. The simulation results proved the superiority of this scheme over other classical methods such as conventional RC. Although the effectiveness of this scheme in tracking the periodic signals and rejecting the unknown disturbances with its two types, this scheme was dependent on continuous parameters such as output, observer states, or state variables. The controller and sensors may experience a lot of communication burden as a result.

For a class of nonlinear systems with time delay, the problems of disturbance rejection and periodic reference tracking under constrained communication resources are addressed by the fourth technique [19]. The effectiveness of the suggested MRC-EID scheme's periodic and aperiodic disturbance rejection has been enhanced, and it has demonstrated favorable tracking performance when dealing with periodic reference signals. Additionally, an FSO-based periodic ETM (PETM) has been developed to build a (FSO-PRTM) that reduces data transmission, conserves communication channels, and uses less energy. The PETM design relied on a static triggering condition even though the control design had superior tracking performance and utilized fewer communication resources while rejecting the two disturbance types. As a result, the static triggering conditions will not be able to adapt when the dynamics of the system change.

The fifth approach focuses on designing a two-dimensional MRC system to achieve high tracking performance for a nonlinear plant [18]. To boost design flexibility, an MRC with two repeating loops is used. Then, the improved RC system's 2D properties are used to build a continuous-discrete 2D model. Utilizing the particle swarm optimization (PSO) technique in order to optimize control and learning activities with low computing complexity and good optimal-solution accuracy, three stability condition parameters must be adjusted and the parameters of the MRC and state-feedback controller are combined optimally. Despite this scheme's efficacy in tracking periodic signals, it is unable to handle unidentified disruptions. Additionally, there is no mechanism for decreasing data transfer, which results in significant energy waste and a burdensome communication load on the controller and sensors.

According to the prior discussions and the deficiencies noted therein, this work examines the construction of EID-based MRC with FSO-based adaptive PETM (FSO-APETM) for the time-delayed T-S fuzzy system. An optimization technique is used to tune the controller parameters and adjust the control and learning actions.

The following is a list of the contributions:

(i) By utilizing the EID estimator, the suggested MRC scheme enhances control performance by effectively compensating for both aperiodic and periodic disturbances besides tracking periodic signals in a defined category of nonlinear systems with time-varying delays. This approach yields comparable results and enhances the overall system performance.

(ii) Considering that the system states are not directly measurable. Due to its straightforward structure and the need for fewer tuning parameters during implementation, an FSO can be utilized to estimate these states.

(iii) The FSO-APETM integrates adaptive triggering conditions, allowing the event-triggered condition to dynamically adjust and adapt to variations in the system dynamics. This adaptive mechanism enhances the efficiency of the triggering process while conserving energy and communication resources.

(iv) The design of EID estimator is independent of the MRC, resulting in a straightforward design process. The simplicity of the procedures allows for a more convenient implementation.

(v) The combination of APETM, EID, MRC, and FSO poses a notable challenge in preserving the stability of the closed-loop system, especially when confronted with nonlinearity and time-varying delay. However, the stability of the overall system is ensured by employing LKF candidate and utilizing the stability criterion of LMIs. Additionally, the proposed controller exhibits robustness against unknown disturbances.

(vi) A PSO algorithm is used to find the appropriate state-feedback control and FSO settings with good optimal-solution accuracy and minimal computational complexity.

2. Problem Statement

The proposed EID technique-based MRC with FSO-APETM for nonlinear systems with time-varying delays that are influenced by unknown aperiodic and periodic disturbances is presented. In addition, using the PSO algorithm, the state feedback controller and FSO parameters are optimized to determine the most effective fusion of gains. The structure of the augmented system which consists of MRC system, FSO-APETM, EID estimator, and T-S fuzzy model under exogenous disturbance is shown in Figure 1.

2.1. T-S Fuzzy Model. Consider a time-varying delay SISO nonlinear system that is susceptible to disturbance input. T-S fuzzy modeling approach can represent nonlinear into r fuzzy plant rules as seen in the following [5]:

If ϕ_1 is N_{1i}, ϕ_2 is N_{2i}, ..., and ϕ_p is N_{pi}, then

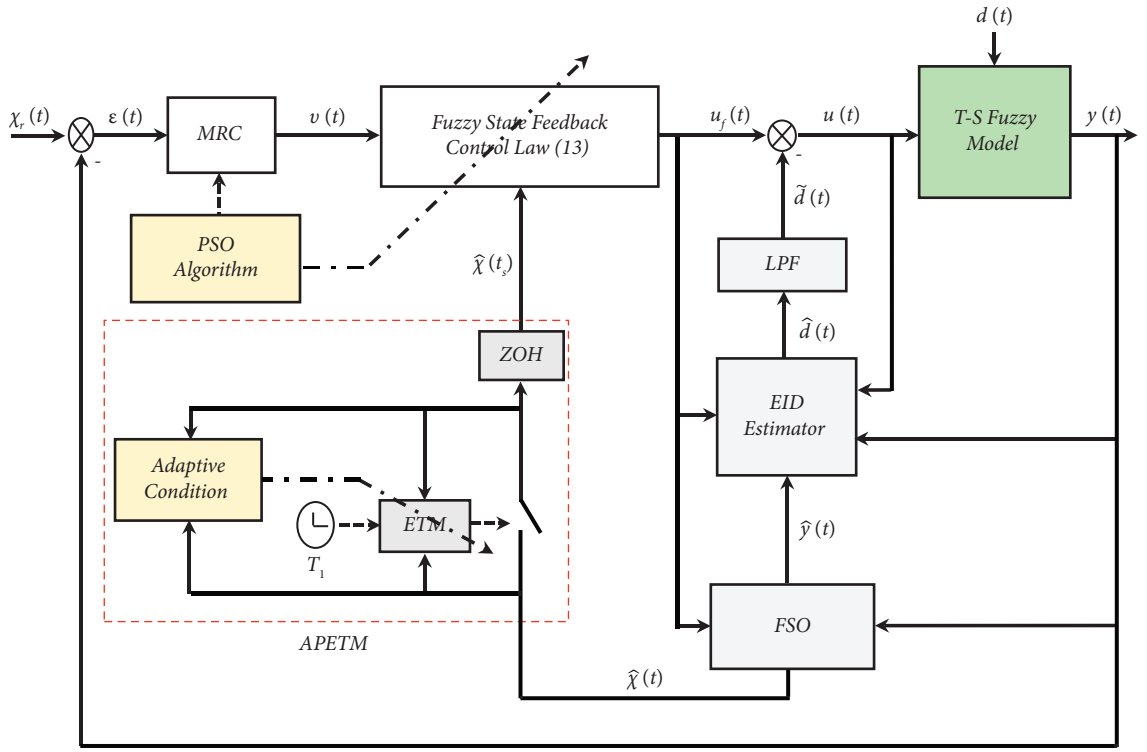

Figure 1: The proposed EID technique with FSO-APETM structure for a class of non-linear systems.

$$\begin{aligned}\dot{\chi}(t) &= A_i\chi(t) + A_{\mathrm{wi}}\chi(t-w(t)) + B_i u(t) + B_{\mathrm{di}}d(t),\\ y(t) &= C_i\chi(t) + D_{\mathrm{vi}}v(t),\\ \chi(t) &= \alpha(t), t \in [-\sigma, 0],\end{aligned} \tag{1}$$

where $\chi(t) \in \mathbb{R}^n$ represents system states, $y(t) \in \mathbb{R}$ is the system output, $u(t) \in \mathbb{R}$ stands for the control input, $v(t) \in \mathbb{R}^q$ is the output noised signal, $d(t) \in \mathbb{R}^q$ is the external disturbances, and $w(t)$ indicates the time-varying delay. Besides, $\alpha(t)$ represents the initial state function. Additionally, A_{di} and $A_i \in \mathbb{R}^{n\times n}$, $B_{\mathrm{wi}} \in \mathbb{R}^{n\times 1}$, $B_i \in \mathbb{R}^{n\times q}$, $D_{\mathrm{vi}} \in \mathbb{R}^q$, and $C_i \in \mathbb{R}^n$ are known matrices. Moreover, $\phi_p(t)$ represents the premise variables; $N_{\mathrm{pi}}, N_{2i}, \ldots, N_{\mathrm{pi}}$ stands for the fuzzy sets. T-S fuzzy model (1) is deduced as following according to the singleton fuzzifier, center average defuzzifier, and product inference:

$$\begin{aligned}\dot{\chi}(t) = \sum_{i=1}^{r} g_i(\phi(t))\big[&A_i\chi(t) + A_{\mathrm{wi}}\chi(t-w(t))\\ &+ B_i u(t) + B_{\mathrm{di}}d(t)\big],\\ y(t) = \sum_{i=1}^{r} g_i(\phi(t))\big[&C_i\chi(t) + D_{\mathrm{vi}}v(t)\big],\end{aligned} \tag{2}$$

where $g_i(\phi(t))$ is the fuzzy weighting function, where $g_i(\phi(t))$ satisfies the conditions; $0 \le g_i(\phi(t)) \le 1$, $\sum_{i=1}^{r} g_i(\phi(t)) = 1$.

2.2. MRC System. The periodic disturbances' rejection and/or periodic signal tracking can be performed using the MRC system. According to Figure 2, the MRC has an LPF, which is described as $l(s)$ before the time-delayed element in positive feedback configuration, where the reference is $x_d(t)$ with T period. A first-order LPF is introduced for the easiest implementation and design. Therefore, $l(s) = w_a/(s + w_a)$, in such $|l(\mathrm{jw})| \approx 1$, in which w_a stands for the cutoff frequency of the LPF. Therefore, the MRC can be characterized as the following state space:

$$\begin{aligned}\dot{\chi}_a(t) &= -w_a\chi_a(t) + w_a\chi_a(t-T) + w_a\varepsilon(t),\\ v(t) &= \chi_a(t-T) + \varepsilon(t),\end{aligned} \tag{3}$$

where the LPF state is $\chi_a(t) \in \mathbb{R}^n$, $v(t)$ stands for output of MRC system, and $\varepsilon(t)$ represents the error in tracking which can be computed as

$$\varepsilon(t) = \chi_r(t) - y(t). \tag{4}$$

2.3. FSO. The system states are estimated using an FSO because it is presumed that they are immeasurable. Based on the parallel distributed compensation (PDC) technique, the system observer dynamics (2) are determined as follows:

If ϕ_1 is N_{1i}, ϕ_2 is $N_{2i}, \ldots$, and ϕ_p is N_{pi}, then

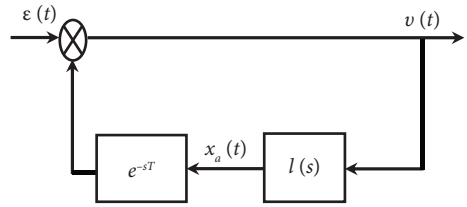

Figure 2: The MRC system configuration.

$$\begin{aligned}\dot{\widehat{\chi}}(t) &= A_i\widehat{\chi}(t) + A_{di}\widehat{\chi}(t-w(t)) + B_i u_f(t)\\ &\quad + \mathscr{L}_i(y(t)-\widehat{y}(t)),\\ \widehat{y}(t) &= C_i\widehat{\chi}(t),\\ \widehat{\chi}(t) &= \widehat{\alpha}(t), t \in [-\sigma, 0].\end{aligned} \tag{5}$$

where $\widehat{y}(t), \widehat{\chi}(t)$ stands for the output and states of the observer, respectively. Moreover, L_i represents the observer gain of the i-th model, and the fuzzy feedback control input is denoted as $u_f(t)$.

To get the overall FSO, we employ the following architecture: center average defuzzifier, singleton fuzzifier, and product inference.

$$\begin{aligned}\dot{\widehat{\chi}}(t) &= \sum_{i=1}^{r} g_i(\phi(t))\left[A_i\widehat{\chi}(t) + A_{di}\widehat{\chi}(t-w(t)) + B_i u_f(t) + L_i(y(t)-\widehat{y}(t))\right],\\ \widehat{y}(t) &= \sum_{i=1}^{r} g_i(\phi(t))\left[C_i\widehat{\chi}(t)\right].\end{aligned} \tag{6}$$

2.4. MRC Based on FSO-APETM. This subchapter starts out by talking about APETM before moving on to MRC based on FSO-APETM. The event detector in Figure 1 samples the observer's states $\widehat{\chi}(t)$ at a fixed interval T_1 in order to watch for an event occurrence. The instants (t_s) of the event triggered can be described as $t_s = i_s T_1$, where $t_s, T_1 \in \mathbb{N}$ with $i_0 = 0$ and $t_s < t_{s+1}$. In addition, $(l_{s,\aleph})$ which characterize the periodic instants can be described by $l_{s,\aleph} = (i_s + \aleph)T_1$ where $\aleph = 0, 1, 2, \ldots, d_s$ with $d_s = i_{s+1} - i_s - 1$. Then, $[t_s, t_{s+1}) = \bigcup_{\aleph=0}^{d_s}[l_{s,\aleph}, l_{s,\aleph+1})$. The condition of ETM is designed using $\varepsilon_o(t)$ which is the error signal of the observer described as [19]:

$$\varepsilon_o(t) = \widehat{\chi}(t_s) - \widehat{\chi}\left(l_{s,\aleph}\right), \quad t \in \left[l_{s,\aleph}, l_{s,\aleph+1}\right). \tag{7}$$

Based on $\varepsilon_o(t)$, the condition of the event-triggering is constructed as

$$\varepsilon_o^T(t)\Theta_1\varepsilon_o(t) \le \epsilon\left(l_{s,\aleph}\right)\widehat{\chi}^T\left(l_{s,\aleph}\right)\Theta_2\widehat{\chi}\left(l_{s,\aleph}\right), \tag{8}$$

where $\epsilon(l_s, \aleph)$ is a time-dependent event-triggered threshold function and $\Theta_1, \Theta_2 > 0$ and symmetric matrices. The following adaption law can be used to update $\epsilon(l_s, \aleph)$:

$$\epsilon\left(l_{s,\aleph+1}\right) = \mathrm{Sat}_{[\underline{\epsilon},\overline{\epsilon}]}\left[\epsilon\left(l_{s,\aleph}\right) + \mathscr{K}\left(\widehat{\chi}^T(t_s)\Theta_1\widehat{\chi}(t_s)\right) - \widehat{\chi}^T\left(l_{s,\aleph}\right)\Theta_2\widehat{\chi}\left(l_{s,\aleph}\right)\right], \epsilon(0) \in [\underline{\epsilon}, \overline{\epsilon}], \tag{9}$$

where $\mathscr{K} > 0$ is a parameter to be adjusted.

$$\mathrm{Sat}_{[\underline{\epsilon},\overline{\epsilon}]}[\chi] = \begin{cases}\overline{\epsilon}, & \chi \ge \overline{\epsilon},\\ \chi, & \underline{\epsilon} \le \chi \le \overline{\epsilon},\\ \underline{\epsilon}, & x \le \underline{\epsilon},\end{cases} \tag{10}$$

where the parameters $\underline{\epsilon}$ and $\overline{\epsilon}$ stand for the lower and upper bounds of $\epsilon(l_{s,\aleph})$, respectively, i.e., the bounds of triggered threshold function, while taking into account the restriction $0 < \underline{\epsilon} \le \overline{\epsilon} < 1$. Current data are provided to ZOH when condition (8) is broken, and hence, the event takes place. If the triggered condition is not met, ZOH retains previous data and event detector continuously samples the observer state $\widehat{x}(t)$. Moreover, $\aleph = 0$, $t_s = l_{s,\aleph}$, and $\varepsilon_o(t)$ are reset to zero with reference to (7). Moreover, condition (8) can be confirmed at the subsequent periodic instant $l_{s,\aleph+1}$. As a result of this ETM, i_{s+1} is computed from

$$i_{s+1} = \min_{\aleph\in\mathbb{N}}\left\{l_{s,\aleph} \,\middle|\, \varepsilon_o^T(t)\Theta_1\varepsilon_o(t) > \epsilon\left(l_{s,\aleph}\right)\widehat{\chi}^T\left(l_{s,\aleph}\right)\Theta_2\widehat{\chi}\left(l_{s,\aleph}\right)\right\}. \tag{11}$$

As a result, the ETM design eliminates the Zeno behavior problem. Define $\tau_s(t) = t - l_{s,\aleph}$, $t \in [l_{s,\aleph}, l_{s,\aleph+1})$, and hence, (7) can be rewritten as follows:

$$\widehat{\chi}(t_s) = \varepsilon_o(t) + \widehat{\chi}(t - \tau_s(t)). \tag{12}$$

The reference $\chi_r(t)$ can be monitored by system output $y(t)$ based on the PDC algorithm. This can be achieved based on the fuzzy rule given below, which depends on signals from the FSO-APETM and MRC.

2.4.1. Control Rule. If ϕ_1 is N_{1j}, ϕ_2 is $N_{2j}, \ldots,$ and ϕ_p is N_{pj}, then

$$u_f(t) = \kappa_{cj} v(t) + \kappa_{pj} \widehat{\chi}(t_s), \tag{13}$$

where κ_{cj} and κ_{pj} are the parameters for the developed fuzzy state feedback controller. In addition, $N_{1j}, N_{2j}, \ldots, N_{\mathrm{pj}}$ are the control fuzzy sets. Hence, fuzzy controller output is deduced from (13) as follows:

$$u_f(t) = \sum_{j=1}^{r} g_j(\phi(t)) \left[\kappa_{\mathrm{cj}} v(t) + \kappa_{\mathrm{pj}} \widehat{\chi}(t_s)\right]. \tag{14}$$

2.5. EID Estimator. By incorporating the EID estimator into the established system, the aperiodic and periodic disturbances together can be reduced. The EID estimation is expressed as follows, as introduced in [12]:

$$\widehat{d}(t) = \sum_{i=1}^{r} h_i(\phi(t)) \left[B_i^{+} \mathscr{L}_i C_i (\chi(t) - \widehat{\chi}(t))\right] + u_f(t) - u(t), \tag{15}$$

with $B_i^{+} = B_i^T / (B_i^T B_i)$. Moreover, the estimated disturbance $\widehat{d}(t)$ may be impacted by the output measurement noise. In order to remove the noise from the estimate, an LPF $f(s)$ is used [12]. The LPF may be set to $f(s) = d_f / (s + d_f)$, where d_f is the LPF cutoff frequency, to make design and usage simple. LPF state space can be formulated as follows:

$$\begin{aligned} \dot{\chi}_f(t) &= A_f \chi_f(t) + B_f \widehat{d}(t), \\ \widetilde{d}(t) &= C_f \chi_f(t), \end{aligned} \tag{16}$$

the filter output and states, respectively, are denoted by $\widetilde{d}(t)$ and $\chi_f(t)$. The combined output of the EID and the state feedback control is used to create the most recent control law, which is

$$u(t) = u_f(t) - \widetilde{d}(t). \tag{17}$$

Remark 1. The periodic disturbance rejection and periodic signal tracking can be just achieved using MRC. Two degrees of freedom are included into the EID-based MRC system to improve control performance for addressing aperiodic and periodic disturbances as well as periodic signal tracking.

With the help of the EID-based MRC in system (1), which is operating under the enhanced feedback control law (17), disturbance attenuation and periodic signal tracking are accomplished with successful way. Furthermore, because of APETM, data updates only occur at predetermined periods, which results in a reduction in communication resources.

2.6. PSO Algorithm. Intelligent optimization methods stochastically and heuristically investigate an ideal solution. They exhibit the traits of a global optimum, high speed, and great precision. The PSO is a metaheuristic method of intelligent optimization that can search a wide range for potential solutions while making little to no assumptions about an optimization problem.

The PSO algorithm finds the appropriate state-feedback control and FSO settings with good optimal-solution accuracy and minimal computational complexity. In order to change the activities for control and learning, it modifies the parameters. To get the T-S based controller in Figure 1 to work well under control, the PSO technique is employed to determine the best set of those parameters. Hence, a PSO method is employed to look for the T-S based MRC system gains.

3. Formation Control Design

The modeling of the entire system is initially presented in this section, after which there is a discussion of the control design analysis for the T-S fuzzy using suggested methodology. Moreover, the parameter optimization is discussed at the last subsection.

3.1. System Modeling. The external disturbance and the periodic reference signal in the suggested design have no effect on the closed-loop system stability. Therefore, creating a state feedback control rule that is unaffected by the disturbance and periodic reference is adequate. Because stability is independent of external signals, external signals are set to zero in the control design technique for simplicity's sake.

Exogenous signals are therefore equal to zero; $v(t) = d(t) = \chi_r(t) = 0$. Consequently, the formulation of the tracking error, in addition to the system state equations, can be redefined as follows:

$$\begin{aligned} \dot{\chi}(t) &= \sum_{i=1}^{r} g_i(\phi(t)) \left[A_i \chi(t) + A_{\mathrm{wi}} \chi(t - w(t)) + B_i u(t)\right], \\ y(t) &= \sum_{i=1}^{r} g_i(\phi(t)) \left[C_i \chi(t)\right], \end{aligned} \tag{18}$$

$$\varepsilon(t) = -\sum_{i=1}^{r} g_i(\varphi(t)) \left[C_i \chi(t)\right]. \tag{19}$$

The following equation describes the estimation error between the observer and system states:

$$\chi_e(t) = \chi(t) - \widehat{\chi}(t). \tag{20}$$

As a result, the augmented system of Figure 1 is characterized by the following formulated state equations that describe the overall system dynamics:

$$\begin{aligned}\dot{\chi}(t) = \sum_{i=1}^{r}\sum_{j=1}^{r} g_i(\varphi(t))g_j(\varphi(t))\Big[\big(A_i - B_i\kappa_{\mathrm{cj}}C_i\big)\chi(t) \\ + A_{\mathrm{wi}}\chi(t-w(t)) + B_i\kappa_{\mathrm{cj}}\chi_a(t-T) + B_i\kappa_{\mathrm{pj}}\chi\big(t-\tau_s(t)\big) \\ - B_i\kappa_{\mathrm{pj}}\chi_e\big(t-\tau_s(t)\big) + B_i\kappa_{\mathrm{pj}}\varepsilon_o(t) - B_iC_f\chi_f(t)\Big],\end{aligned} \tag{21}$$

$$\dot{\chi}_e(t) = \sum_{i=1}^{r}\sum_{j=1}^{r} g_i(\varphi(t))g_j(\varphi(t))\Big[(A_i - \mathscr{L}_iC_i)\chi_e(t) + A_{\mathrm{wi}}\chi_e(t-w(t)) - B_iC_f\chi_f(t)\Big], \tag{22}$$

$$\dot{\chi}_a(t) = \sum_{i=1}^{r} g_i(\varphi(t))\big[-w_a\chi_a(t) + w_a\chi_a(t-T) - w_aC_i\chi(t)\big], \tag{23}$$

and

$$\dot{\chi}_f(t) = \sum_{i=1}^{r} g_i(\varphi(t))\Big[B_fB_i^{+}\mathscr{L}_iC_i\chi_e(t) + \big(A_f + B_fC_f\big)\chi_f(t)\Big]. \tag{24}$$

Therefore, equations (21)–(24) describe the overall system of Figure 1.

3.2. Analysis of Stability and Control Gain Design. The entire system stability is examined in this paragraph using the LKF theory and the presumptions are listed below:

The LKF theory and the following suppositions are used in this subsection for the stability analyses of the overall system:

Assumption 2. For asymptotic stability and perfect performance tracking, system (1) is anticipated to be observable and controllable.

Assumption 3 (see [19]). Suppose that $B_i \in \mathbb{R}^{n\times m}$ is a matrix of rank m. Thus, the SVD of B_i is as

$$B_i = \Upsilon\begin{bmatrix}\Lambda\\ 0\end{bmatrix}\vartheta^T. \tag{25}$$

where Υ and ϑ are unitary matrices and Λ is a diagonal matrix.

Lemma 4 (see [19]). *Based on the SVD (25), there is a matrix $\overline{\chi}$ that meets the equality; $\chi B_i = B_i\overline{\chi}$ and that holds if*

$$\chi = \Upsilon\,\mathrm{diag}\{\chi_{11}, \chi_{22}\}\Upsilon^T, \tag{26}$$

Lemma 5 (see [22]). *Any constant matrices G and Y are subject to the following inequality:*

$$G + \epsilon(t)Y < 0, \tag{27}$$

for $\underline{\epsilon} \le \epsilon(t) \le \overline{\epsilon}$, if and only if

$$G + \underline{\epsilon}Y < 0, G + \overline{\epsilon}Y < 0. \tag{28}$$

In terms of LMIs, the following theorem determines the requirement of closed-loop system stability.

Theorem 6. *By considering the positive definite matrices $\mathscr{P}_1, \mathscr{P}_2, \mathscr{P}_3, \mathscr{P}_4, \varsigma_1, \varsigma_2, \mu, \Gamma, \Theta_1, \Theta_2, \psi_1, \psi_2, \psi_3$ and arbitrary matrices $\widehat{F}_1, \widehat{F}_2, \widehat{F}_3, \zeta_{1i}, \zeta_{2j}, \zeta_{3j}, \zeta_{4i}$ of appropriate dimensions, with the constant parameters $T, T_1, \lambda, \overline{\epsilon}, w_f$ and positive tuning parameters γ, β, α and w_a, the following LMIs hold:*

$$\begin{aligned}F_1 &= \begin{bmatrix}\psi_3 & \widehat{F}_3 & 0\\ * & \beta e^{-\beta T_1}\varsigma_2 & 0\\ * & * & \gamma e^{-\gamma T_1}\mu\end{bmatrix} \ge 0,\\ F_2 &= \begin{bmatrix}F_{2.1} & F_{2.2}\\ * & F_{2.3}\end{bmatrix} \ge 0,\end{aligned} \tag{29}$$

where $F_{2.1} = diag\ \{\psi_1, \psi_2\}, F_{2.2} = diag\ \{\widehat{F}_1, \widehat{F}_2\}, F_{2.3} = diag\ \{\alpha e^{-\alpha T_1}\varsigma_1, 0\}$

$$\Sigma = \begin{bmatrix}\Sigma_1 & \Sigma_2\\ * & \Sigma_3\end{bmatrix} < 0, \tag{30}$$

where $\Sigma_1 = \begin{bmatrix}\Sigma_{1.1} & \Sigma_{1.2}\\ * & \Sigma_{1.3}\end{bmatrix}$, $\Sigma_2 = \begin{bmatrix}\Sigma_{2.1} & \Sigma_{2.2}\\ 0 & \Sigma_{2.3}\end{bmatrix}$, $\Sigma_3 = \begin{bmatrix}\Sigma_{3.1} & \Sigma_{3.2}\\ * & \Sigma_{3.3}\end{bmatrix}$,

$$\Sigma_{1.1}=\begin{bmatrix}\mathrm{sym}\{\mathscr{P}_1A_i-B_i\zeta_{2j}C_i\} & 0 & -\omega_a\mathscr{P}_3C_i\\ * & \mathrm{sym}\{\mathscr{P}_2A_i-\zeta_{1i}C_i\} & 0\\ * & * & -2\omega_a\mathscr{P}_3+\Xi\end{bmatrix},$$

$$\Sigma_{1.2}=\begin{bmatrix}-\mathscr{P}_1B_iC_f & B_i\zeta_{3j}+\widehat{F}_1^T & -B_i\zeta_{3j}\\ -\mathscr{P}_2B_iC_f+B_fB_i^+\zeta_{4i}C_i & 0 & \widehat{F}_2^T\\ 0 & 0 & 0\end{bmatrix},$$

$$\Sigma_{1.3}=\begin{bmatrix}\mathrm{sym}\{\mathscr{P}_4A_f+\mathscr{P}_4B_fC_f\} & 0 & 0\\ * & -sym\{\widehat{F}_1\}+T_1\psi_1+\overline{\varepsilon}\Theta_2 & 0\\ * & * & -sym\{\widehat{F}_2\}+T_1\psi_2+\overline{\varepsilon}\Theta_2\end{bmatrix},$$

$$\Sigma_{2.1}=\begin{bmatrix}-\mathscr{P}_2A_{\mathrm{d}i}+\widehat{F}_3^T & B_i\zeta_{2j} & B_i\zeta_{3j}\\ \mathscr{P}_2A_{\mathrm{d}i} & 0 & 0\\ 0 & \omega_a\mathscr{P}_3 & 0\end{bmatrix},$$

$$\Sigma_{2.2}=\begin{bmatrix}\mathscr{P}_1A_i-B_i\zeta_{2j}C_i & 0 & 0\ 0\\ 0 & \mathscr{P}_2A_i-\zeta_{1i}C_i & 0\ 0\\ 0 & 0 & 0\ 0\end{bmatrix},\tag{31}$$

$$\Sigma_{2.3}=\begin{bmatrix}-\mathscr{P}_1B_iC_f & -\mathscr{P}_2B_iC_f & 0\ 0\\ B_i\zeta_{3j} & 0 & 0\ 0\\ -B_i\zeta_{2j} & 0 & 0\ 0\end{bmatrix},$$

$$\Sigma_{3.1}=\begin{bmatrix}-\mathrm{sym}\{\widehat{F}_3\}+\sigma\psi_3 & 0 & 0\\ * & -\Xi & 0\\ * & * & -\Theta_1\end{bmatrix},$$

$$\Sigma_{3.2}=\begin{bmatrix}\mathscr{P}_1A_{\mathrm{d}i} & \mathscr{P}_2A_{\mathrm{d}i} & 0\ 0\\ B_i\zeta_{2j} & 0 & 0\ 0\\ B_i\zeta_{3j} & 0 & 0\ 0\end{bmatrix},$$

$$\Sigma_{3.3}=\begin{bmatrix}-\mathrm{sym}\{\mathscr{P}_1\}+\psi_1+\psi_2 & 0 & 0 & 0\\ * & -\mathrm{sym}\{\mathscr{P}_2\}+\mu & 0 & 0\\ * & * & -\varsigma_2(1-\Xi)e^{-\beta\sigma} & 0\\ * & * & * & -\mu(1-\Xi)e^{-\gamma\sigma}\end{bmatrix}.$$

Therefore, the asymptotic stability of the system is achieved. After that, the following equations can be used to compute the observer and controller parameters in accordance with the solved LMIs:

$$\mathscr{L}_i=\mathscr{P}_2^{-1}\zeta_{1i},\tag{32}$$

$$\kappa_{\mathrm{pj}}=\overline{\mathscr{P}}_1^{-1}\zeta_{3j},\tag{33}$$

$$\kappa_{\mathrm{cj}}=\overline{\mathscr{P}}_1^{-1}\zeta_{2j},\tag{34}$$

Proof. By selecting a LKF candidate as described

$$\mathscr{V}(t)=\sum_{i=1}^{4}\mathscr{V}_i(t),\tag{35}$$

where

$$\mathscr{V}_1(t) = \chi^T(t)\mathscr{P}_1\chi(t) + \int_{t-\tau_s(t)}^{t} e^{\alpha(s-t)}\dot{\chi}^T(s)\varsigma_1\dot{\chi}(s)\mathrm{d}s + \int_{t-w(t)}^{t} e^{\beta(s-t)}\dot{\chi}^T(s)\varsigma_2\dot{\chi}(s)\mathrm{d}s, \tag{36}$$

$$\mathscr{V}_2(t) = \chi_e^T(t)\mathscr{P}_2\chi_e(t) + \int_{t-w(t)}^{t} e^{\gamma(s-t)}\dot{\chi}_e^T(s)\mu\dot{\chi}_e(s)\mathrm{d}s, \tag{37}$$

$$\mathscr{V}_3(t) = \chi_a^T(t)\mathscr{P}_3\chi_a(t) + \int_{t-T}^{t} \chi_a{}^T(s)\Xi\chi_a(s)\mathrm{d}s, \tag{38}$$

$$\mathscr{V}_4(t) = \chi_f^T(t)\mathscr{P}_4\chi_f(t). \tag{39}$$

The derivative of the function $\mathscr{V}(t)$ can be calculated using the following expression:

$$\dot{\mathscr{V}}(t) = \sum_{i=1}^{4}\dot{\mathscr{V}}_i(t), \tag{40}$$

where

$$\begin{aligned}\dot{\mathscr{V}}_1(t) \le & \sum_{i=1}^{r}\sum_{j=1}^{r} g_i(\varphi(t))g_j(\varphi(t))2\chi^T(t)\left(\mathscr{P}_1A_i - \mathscr{P}_1B_i\kappa_{\mathrm{cj}}C_i\right)\\ & \times\chi(t) + 2\chi^T(t)\mathscr{P}_1A_{\mathrm{di}}\chi(t-w(t)) + 2\chi^T(t)\mathscr{P}_1B_i\kappa_{\mathrm{pj}}\chi\left(t-\tau_s(t)\right)\\ & - 2\chi^T(t)\mathscr{P}_1B_i\kappa_{\mathrm{pj}}\chi_e\left(t-\tau_s(t)\right) + 2\chi^T(t)\mathscr{P}_1\\ & \times B_i\kappa_{\mathrm{cj}}\chi_a(t-T) + 2\chi^T(t)\mathscr{P}_1B_i\kappa_{\mathrm{pj}}\varepsilon_o(t) - 2\chi^T(t)\mathscr{P}_1\\ & \times B_iC_f\chi_f(t) + \dot{\chi}^T(t)\left(\varsigma_1+\varsigma_2\right)\dot{\chi}(t) - (1-\lambda)e^{-\beta\sigma}\dot{\chi}^T(t-d(t))\\ & \varsigma_2\dot{\chi}(t-w(t)) - \alpha\int_{t-\tau_s(t)}^{t} e^{\alpha(s-t)}\dot{\chi}^T(s)\varsigma_1\dot{\chi}(s)\mathrm{d}s\\ & - \beta\int_{t-w(t)}^{t} e^{\beta(s-t)}\dot{\chi}^T(s)\varsigma_2\dot{\chi}(s)\mathrm{d}s,\end{aligned} \tag{41}$$

$$\begin{aligned}\dot{\mathscr{V}}_2(t) \le & \sum_{i=1}^{r}\sum_{j=1}^{r} g_i(\varphi(t))g_j(\varphi(t))2\chi_e^T(t)\left(\mathscr{P}_2A_i - \mathscr{P}_2\mathscr{L}_iC_i\right)\\ & \times\chi_e(t) + 2\chi_e^T(t)\mathscr{P}_2A_{\mathrm{di}}x_e(t-w(t)) - 2\chi_e^T(t)\mathscr{P}_2B_i\\ & \times C_f\chi_f(t) + \dot{x}_e^T(t)\mu\dot{\chi}_e(t) - (1-\lambda)e^{-\gamma\sigma}\dot{\chi}_e^T(t-w(t))\\ & \times\mu\dot{\chi}_e(t-w(t)) - \gamma\int_{t-w(t)}^{t} e^{\gamma(s-t)}\dot{\chi}_e^T(s)\mu\dot{\chi}_e(s)\mathrm{d}s,\end{aligned} \tag{42}$$

$$\begin{aligned}\dot{\mathscr{V}}_3(t) = & \sum_{i=1}^{r} g_i(\varphi(t))\chi_a^T(t)\left(-2\omega_a\mathscr{P}_3 + \Xi\right)\chi_a(t) - 2\omega_a\chi_a^T(t)\\ & \times\mathscr{P}_3C_i\chi(t) + 2\omega_a\chi_a^T(t)\mathscr{P}_3\chi_a(t-T)\\ & - \chi_a^T(t-T)\Xi\chi_a(t-T),\end{aligned} \tag{43}$$

$$\dot{\mathscr{V}}_4(t) = \sum_{i=1}^{r} g_i(\varphi(t)) 2\chi_f^T(t)\left(\mathscr{P}_4 A_f + \mathscr{P}_4 B_f C_f\right)\chi_f(t) + 2\chi_f^T(t)\mathscr{P}_4 B_f B_i^{+}\mathscr{L}_i C_i \chi_e(t). \tag{44}$$

Based on Newton–Leibniz expression, which is explained as

$$\chi(t) - \chi\left(t-\tau_s(t)\right) - \int_{t-\tau_s(t)}^{t} \dot{\chi}(s)\mathrm{d}s = 0. \tag{45}$$

Therefore, it is possible to establish the following equality:

$$\begin{aligned} 2\chi^T\left(t-\tau_s(t)\right)\widehat{F}_1\left[\chi(t) - \chi\left(t-\tau_s(t)\right) - \int_{t-\tau_s(t)}^{t}\dot{\chi}(s)\mathrm{d}s\right] &= 0,\\ 2\chi_e^T\left(t-\tau_s(t)\right)\widehat{F}_2\left[\chi_e(t) - \chi_e\left(t-\tau_s(t)\right) - \int_{t-\tau_s(t)}^{t}\dot{\chi}_e(s)\mathrm{d}s\right] &= 0,\\ 2\chi^T\left(t-w(t)\right)\widehat{F}_3\left[\chi(t) - \chi\left(t-w(t)\right) - \int_{t-\tau_s(t)}^{t}\dot{\chi}(s)\mathrm{d}s\right] &= 0, \end{aligned} \tag{46}$$

Also, from (21) and (22), we have

$$\begin{aligned} &2\dot{\chi}^T(t)\mathscr{P}_1\sum_{i=1}^{r}\sum_{j=1}^{r} g_i(\varphi(t))g_j(\varphi(t))\Big[\left(A_i - B_i\kappa_{\mathrm{cj}}C_i\right)\chi(t)\\ &\quad + A_{\mathrm{d}i}x\left(t-w(t)\right) + B_i\kappa_{\mathrm{cj}}\chi_a(t-T) + B_i\kappa_{\mathrm{pj}}\chi\left(t-\tau_s(t)\right)\\ &\quad - B_i\kappa_{\mathrm{pj}}\chi_e\left(t-\tau_s(t)\right) + B_i\kappa_{\mathrm{pj}}\varepsilon_o(t) - B_iC_f\chi_f(t)\\ &\quad - \dot{\chi}(t)\Big] = 0,\\ &2\dot{\chi}_e^T(t)\mathscr{P}_2\sum_{i=1}^{r}\sum_{j=1}^{r} g_i(\varphi(t))g_j(\varphi(t))\Big[\left(A_i - \mathscr{L}_iC_i\right)x_e(t)\\ &\quad + A_{\mathrm{d}i}\chi_e\left(t-w(t)\right) - B_iC_f\chi_f(t) - \dot{\chi}_e(t)\Big] = 0. \end{aligned} \tag{47}$$

Furthermore,

$$\begin{aligned} \tau_s(t)\chi^T\left(t-\tau_s(t)\right)\psi_1\chi\left(t-\tau_s(t)\right) - \int_{t-\tau_s(t)}^{t}\chi^T\left(t-\tau_s(t)\right)\times\psi_1\chi\left(t-\tau_s(t)\right)\mathrm{d}s &= 0,\\ \tau_s(t)\chi_e^T\left(t-\tau_s(t)\right)\psi_2 x_e\left(t-\tau_s(t)\right) - \int_{t-\tau_s(t)}^{t}\chi_e^T\left(t-\tau_s(t)\right)\times\psi_2\chi_e\left(t-\tau_s(t)\right)\mathrm{d}s &= 0,\\ w(t)\chi^T\left(t-w(t)\right)\psi_3\chi\left(t-w(t)\right) - \int_{t-w(t)}^{t}\chi^T\left(t-w(t)\right)\psi_3\chi\left(t-w(t)\right)\mathrm{d}s &= 0. \end{aligned} \tag{48}$$

By replacing $\epsilon(l_{s,J})$ with $\bar{\epsilon}$ in the condition (8), which is reformulated as

$$-\varepsilon_o^T(t)\Theta_1\varepsilon_o(t) + \bar{\epsilon}\chi^T\left(t-\tau_s(t)\right)\Theta_2\chi\left(t-\tau_s(t)\right) + \bar{\epsilon}\chi_e^T\left(t-\tau_s(t)\right)\Theta_2\chi_e\left(t-\tau_s(t)\right) - 2\bar{\epsilon}\chi^T\left(t-\tau_s(t)\right)\Theta_2\chi_e\left(t-\tau_s(t)\right). \tag{49}$$

After that, we plug $\mathscr{P}_2L_i = \zeta_{1i}$ into the previous equations. Following that, a matrix $\overline{\mathscr{P}}_1$ satisfies the following equality based on Assumption 3 and Lemma 4:

$$\mathscr{P}_1B_i = B_i\overline{\mathscr{P}}_1. \tag{50}$$

In addition, there is a matrix $\overline{\mathscr{P}}_4$ that satisfies

$$\mathscr{P}_4B_i = B_i\overline{\mathscr{P}}_4. \tag{51}$$

Assume $\mathscr{P}_1 = \Upsilon\ \mathrm{diag}\ \{\mathscr{P}_{11}, \mathscr{P}_{22}\}\Upsilon^T$, then we have $\overline{\mathscr{P}}_1 = \vartheta\Lambda^{-1}\mathscr{P}_{11}\Lambda\vartheta^T$, and assume $\mathscr{P}_4 = \Upsilon\ \mathrm{diag}\ \{\mathscr{P}_{41}, \mathscr{P}_{44}\}\Upsilon^T$, then we have $\overline{\mathscr{P}}_4 = \vartheta\Lambda^{-1}\mathscr{P}_{41}\Lambda\vartheta^T$. Then, by substituting $\zeta_{2j} = \overline{\mathscr{P}}_1\kappa_{\mathrm{cj}}$, $\zeta_{3j} = \overline{\mathscr{P}}_1\kappa_{\mathrm{pj}}$, and $\zeta_{4i} = \overline{\mathscr{P}}_4\mathscr{L}_i$ into the preceding

equations and adding the equations be resulted; (41)–(44) and (46)–(49), and hence, the $\mathscr{V}(t)$ derivative is estimated to

$$\begin{aligned}\dot{\mathscr{V}}(t) \le & \sum_{i=1}^{r}\sum_{j=1}^{r} g_i(\varphi(t))g_j(\theta(t))\left[\Omega^T(t)\chi\Omega(t)\right] \\ & - \int_{t-w(t)}^{t} {\Pi_1}^T(t,s)_{F_1}\Pi_1(t,s)\mathrm{d}s \\ & - \int_{t-\tau_s(t)}^{t} {\Pi_2}^T(t,s)_{F_2}\Pi_2(t,s)\mathrm{d}s,\end{aligned} \tag{52}$$

where ${\Pi_1}^T(t,s) = [\chi^T(t-w(t)), \dot{\chi}^T(s), {\dot{\chi}_e}^T(s)]$, ${\Pi_2}^T(t,s) = [\chi^T(t-\tau_s(t)), \chi_e^T(t-\tau_s(t)), \dot{\chi}^T(s), \dot{\chi}_e^T(s)]$, $\Omega^T(t) = [\chi^T(t), \chi_e^T(t), \chi_a^T(t), \chi_f^T(t), \chi^T(t-\tau_s(t)), \chi_e^T(t-\tau_s(t)), \chi^T(t-w(t)), \chi_a^T(t-T), \varepsilon_o^T(t), \dot{\chi}^T(t), {\dot{\chi}_e}^T(t), \dot{\chi}(t-w(t)), \dot{\chi}_e(t-w(t))]$. Furthermore, F_1, F_2 can be produced as in (29) and Σ is identical to (30).

According to Lemma 5, $\Sigma = \widetilde{\Sigma} + \epsilon(l_{s,j})\widetilde{\widetilde{\Sigma}} < 0$ applies to $\Sigma = \widetilde{\Sigma} + \underline{\epsilon}\widetilde{\widetilde{\Sigma}} < 0$, $\Sigma = \widetilde{\Sigma} + \overline{\epsilon}\widetilde{\widetilde{\Sigma}} < 0$. For $\widetilde{\widetilde{\Sigma}} > 0$, the following inequity exists: $\widetilde{\Sigma} + \underline{\epsilon}\widetilde{\widetilde{\Sigma}} \le \widetilde{\Sigma} + \overline{\epsilon}\widetilde{\widetilde{\Sigma}}$.

So, Σ is equivalent to $\widetilde{\Sigma} + \overline{\epsilon}\widetilde{\widetilde{\Sigma}}$ and (30). Therefore, if $\Sigma < 0, F_1$ and $F_2 \ge 0$, as a result, $\dot{V}(t) < 0$, ensuring the system's asymptotic stability. This completes the proof, and then the parameters $\mathscr{L}_i, \kappa_{\mathrm{pj}}$ and κ_{cj} may be obtained as (32)–(34), respectively. □

3.2.1. Design Algorithm. To obtain the best feedback controller and observer parameters, the following steps can be used:

Step 1: calculate the period T of the time delay element corresponding to MRC. In addition, for the LPF $l(s)$, we compute the cutoff frequency w_a, in which the conditions of $l(s)$ in subsection B of section II can be satisfied.

Step 2: for the LPF $f(s)$, we choose the matrices A_f, B_f, and C_f so that they satisfy the conditions in subsection E of section II.

Step 3: set the APETM sample time (T_1) and the triggered threshold function bounds, i.e., $\underline{\epsilon}, \overline{\epsilon}$.

Step 4: based on the positive tuning parameters α, β, and γ, the LMI Matlab toolbox can be used to find a workable solution to LMI (30).

Step 5: as a result and based on (32)–(34), the parameters $L_i, \kappa_{\mathrm{pj}}$ and κ_{cj} can be obtained, respectively.

3.3. Parameter Optimization. The PSO is a metaheuristic algorithm because it searches a huge number of potential solutions while making few or no assumptions about an optimization issue. Hence, a PSO method is employed to look for the T-S based MRC system gains. The optimization of tuning parameters in an LKF is turned into the design of the MRC and controller parameters. To ensure that the T-S based MRC system performs well under management, the optimal possible combination of those parameters is found using the PSO algorithm under an LMI-based stability condition. In order to balance the control and learning acts, we must devise a combination of w_a, γ, β, and α.

Because of the independently of these parameters for each other, their connection makes parameter selection challenging. Finding a method to pick optimal settings is so important in both theory and practice. Intelligent optimization methods are rapid, efficient, and accurate. It gives us a way to deal with this issue.

3.3.1. PSO Algorithm. In order to evaluate the PSO algorithm's performance, the following cost function developed in [25] is chosen:

$$J_i^l = 0.5 * \sum_{\aleph=1}^{K}\left[\int_{(\aleph-1)T}^{\aleph T} \varepsilon_i^2(t)d(t)\right], \tag{53}$$

where $\varepsilon_i(t)$ and J_i are the errors in tracking and performance index of i^{th} particle, respectively. Moreover, K is the repetitive periods' number. The optimization challenge covered in this study is to identify LMI (30) settings that minimize (53). The velocity and position updating laws are

$$\begin{aligned}\delta_i^l &= a\varrho_i^{l-1} + b_1 d_1\left(\varrho_{pi}^{l-1} - \varrho_i^{l-1}\right) + b_2 d_2\left(\varrho_g^{l-1} - \varrho_i^{l-1}\right), \\ \varrho_i^l &= \varrho_i^{l-1} + \delta_i^l.\end{aligned} \tag{54}$$

In (54), $\varrho_i = [w_{\mathrm{ai}}, \Upsilon_i, \epsilon_i]$ is the i^{th} particle's current value and δ_i is its current velocity. In addition, a is an inertia weight, d_1 and d_2 are distributed vectors in $[0, 1)$, and l is the iterations' number. Furthermore, the global and prior learning coefficients are represented by b_1 and b_2, respectively. Besides, ϱ_g is the particle's global optimal value, and ϱ_{pi} is the i^{th} particle's prior optimal value.

4. Simulation Results

In this section, the effectiveness and superiority of the proposed APETM-MRC-based EID with the PSO algorithm are illustrated through the application of a numerical example within the context of a T-S fuzzy system that is provided in [25].

Example 1. Using the following parameters, let us examine the T-S fuzzy system (2):

$$\begin{aligned} A_1 &= \begin{bmatrix} -1 & 3 \\ 2 & -3 \end{bmatrix}, \\ A_2 &= \begin{bmatrix} -1 & 2 \\ 2 & -3.5 \end{bmatrix}, \\ A_{w1} &= \begin{bmatrix} 5 & -1 \\ -2 & -3 \end{bmatrix}, \\ A_{w2} &= \begin{bmatrix} 4 & -1 \\ -1.5 & 0 \end{bmatrix}, \\ B_1 &= B_2 \\ &= \begin{bmatrix} 1 \\ 0 \end{bmatrix}, \text{and} \\ C_1 &= C_2 \\ &= \begin{bmatrix} 5 & 0 \end{bmatrix}. \end{aligned} \tag{55}$$

Take into account that the input signal is $\chi_r(t) = \sin(\pi t), \forall t > 0$ and exogenous disturbances are $d_1(t) = \sin(\pi t)$,

$$d_2(t) = \begin{cases} 0.4\,(10\sin(\pi t) + 1.5\tan h\,(t-27) + 13\tan h\,(t-37)), & 20 \le t \le 35s, \\ 0, & \text{elsewhere}, \end{cases} \tag{56}$$

as periodic and aperiodic disturbances, respectively. Additionally, we consider the delay which is varying with time as $w(t) = 0.5 + 0.5\sin(t)$. Moreover, we choose $w_a = 100$ rad/sec for MRC filter and $w_f = 100$ of the EID filter. The membership functions are chosen to be

$$\begin{aligned} h_1(\chi(t)) &= 0.5\,(1 - \cos(\chi_1(t))), \\ h_2(\chi(t)) &= 0.5\,(1 + \cos(\chi_1(t))). \end{aligned} \tag{57}$$

By using the values of other parameters as $\alpha = 0.4, \beta = 0.2, \gamma = 0.6, \underline{\epsilon} = 0.01, \overline{\epsilon} = 0.5, \mathscr{K} = 0.1, T_1 = 1$ sec, and $\Theta_1 = \Theta_2 = I_{2\times 2}$.

Next, we chose the parameters' search ranges for the PSO algorithm as $\epsilon \in (1, 50), \Upsilon \in (0, 1), w_a \in [0, 1), K = 30, n = 30$, $b_1 = 1$, $b_2 = 1.2, a = 0.5$, and $J_{\text{set}} = 10^{-3}$ The least cost function and the tuning parameters were combined in the PSO algorithm in the best possible way, where $w_a = 0.458$, $\epsilon = 35.61, \Upsilon = 0.001$, and $J = 1.25 * 10^{-4}$. As demonstrated in Theorem 6, by resolving the LMIs, fuzzy state feedback and FSO parameters are realized as follows: $\kappa_{p1} = [\,189.254 \quad -5.521\,], \kappa_{p2} = [\,154.651 \quad -4.352\,], \kappa_{c1} = 85.540$, $\kappa_{c2} = 34.56, L_1 = [\,2.254 \quad -4.635\,]^T$, and $L_2 = [\,16.24 \quad -2.954]^T$. The initial conditions have been taken to be $\chi^T(0) = [\,-0.5 \quad 0.3\,]$. In addition, we go over the system and reference responses in the subsequent situations.

4.1. Case 1: System under MRC Based on T-S Fuzzy (without APETM and EID Technique) [5] and System under the Proposed Controller. Figure 3 illustrates the tracking efficiency for the output trajectories of the closed-loop system using and without an EID technique. Good tracking performance has been reached in this case without the usage of an EID estimator. However, during the $20 - 35$ second aperiodic disturbance interval, the tracking error is larger and its amplitude has reached to a value of 0.5, and after the aperiodic disruption, the stable state has been reached, as displayed in Figure 3(b). In contrast, using the suggested controller, the output $y(t)$ goes in the direction of the signal $\chi_r(t)$ with a minimum tracking error and without overshoot. Compared to the system without EID, steady state was reached more quickly. In addition to compensating for periodic disturbances, the control system can also handle aperiodic ones, where the maximum tracking error reached 0.05.

4.2. Case 2: System under MRC Based on T-S Fuzzy with EID Estimator [25] and the System under Proposed Controller. Figure 4 shows the input $\chi_r(t)$ and system output $y(t)$ state responses over time. Compared to the traditional MRC, both controllers have efficiently attenuated both aperiodic and periodic disturbances. However, the system under the proposed controller has the least tracking error as displayed in Figure 4(b).

As seen in Figure 5, the importance of the suggested controller may be seen in the communication resources it saves. The time span between two sequential event triggering instants for the data transmission is shown in Figure 5. In contrast to the other system where the control activities are constantly updated, only updating the control actions when necessary can help in saving on computing and communication resources.

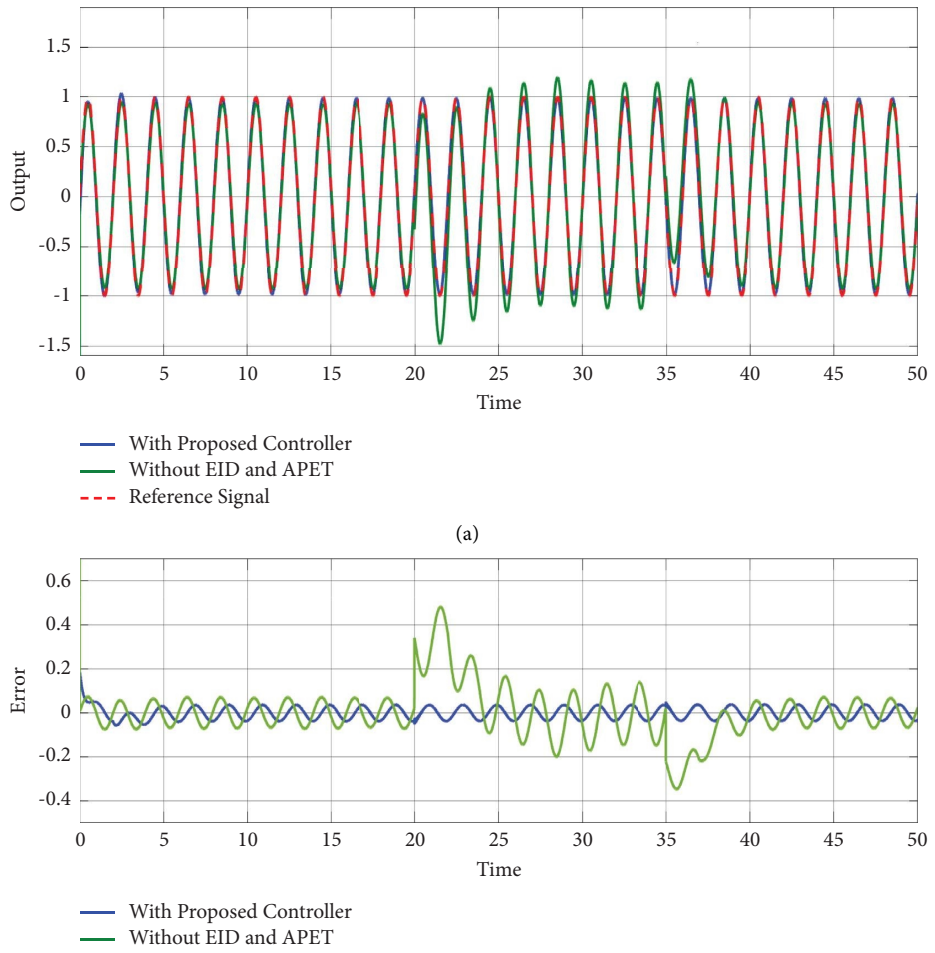

Figure 3: System tracking responses under T-S Fuzzy based MRC system [5] and proposed controller: (a) $y(t)$. (b) $\varepsilon(t)$.

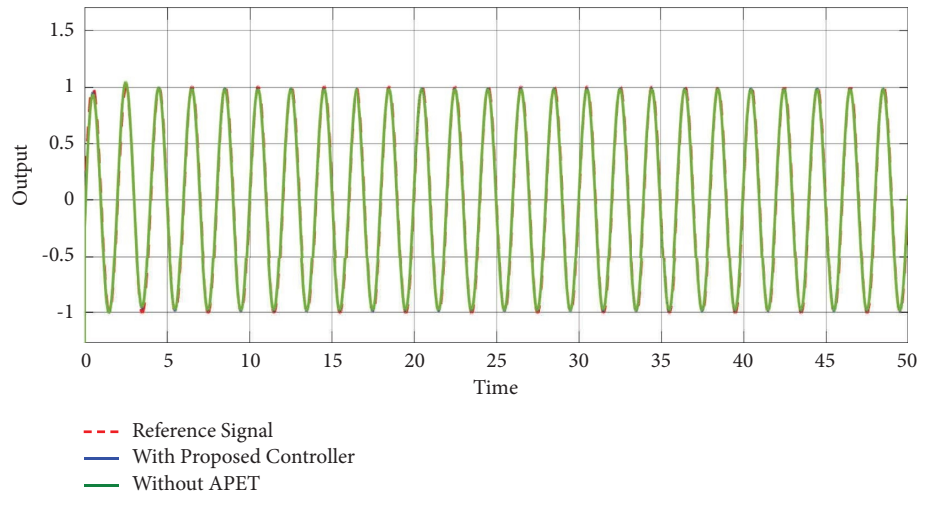

Figure 4: Continued.

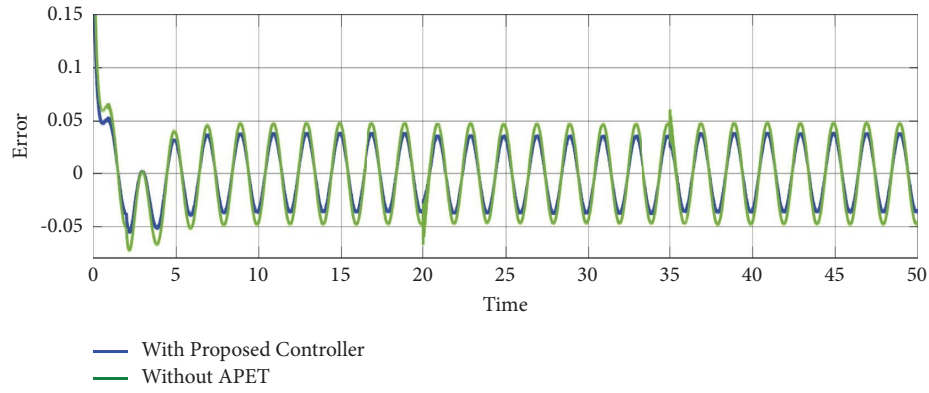

(b)

Figure 4: System tracking responses under T-S Fuzzy based MRC system based on EID [25] and proposed controller: (a) $y(t)$. (b) $\varepsilon(t)$.

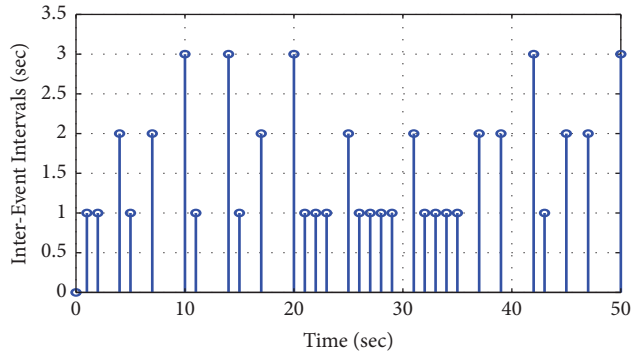

Figure 5: The time between events under APETM.

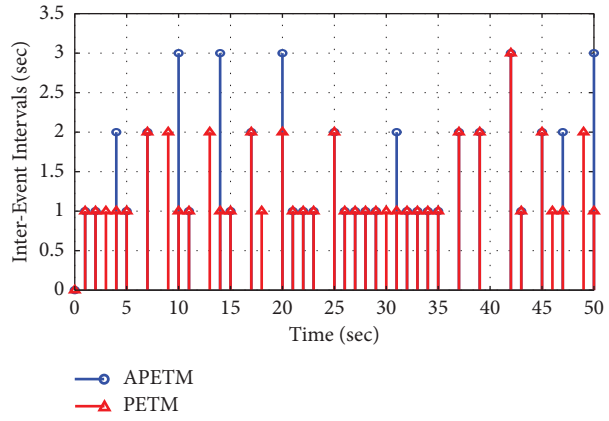

Figure 6: The time between events under PETM [19] and APETM (proposed).

4.3. Case 3: System under MRC Based on T-S Fuzzy with EID Estimator-Based PETM [19] and System under the Proposed Controller. As seen in Figure 6, the suggested controller's importance may be seen in its ability to conserve communication resources. The suggested APETM and the traditional PETM's data transmission interevent intervals are contrasted in Figure 6. It is observed that the suggested APETM has minimum triggering times which are 34 in comparison with PETM which is 40 times. As a result, interevent intervals are longer in the APETM than in the PETM, and the amount of communication resources saved is directly correlated with the length of these intervals. The amount of communication and processing resources saved increases with the interevent delay. As a result, it may be said that APETM is more effective than traditional PETM at reducing data transmission frequency and using less communication resources overall.

Table 1 utilizes four performance indices to compare the following: the MRC scheme based on the T-S fuzzy system without the EID technique, the MRC scheme incorporating the EID technique with the T-S fuzzy model, and the proposed controller. The performance indices considered are the mean absolute error (MAE), the mean square error

Table 1: Comparison results.

Comparison	Reference [5]	Reference [25]	Proposed controller
MAE	0.0820	0.0745	0.0251
MSE	0.0139	0.0092	0.0012
RMSE	0.1180	0.0959	0.0347
S.D	0.0848	0.0457	0.0240

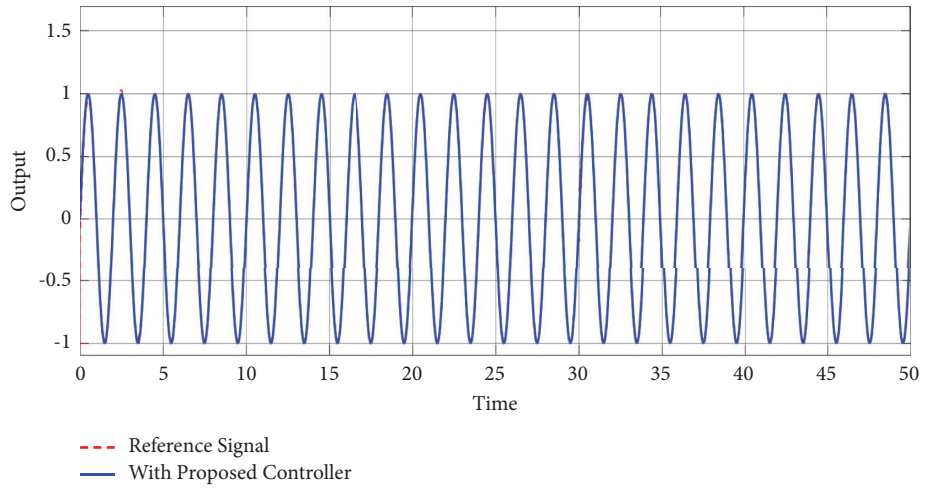

(a)

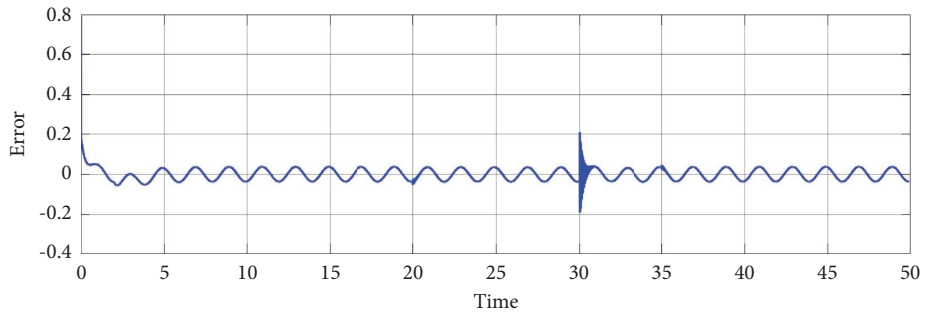

(b)

Figure 7: System output under input disturbance. (a) Output. (b) Error.

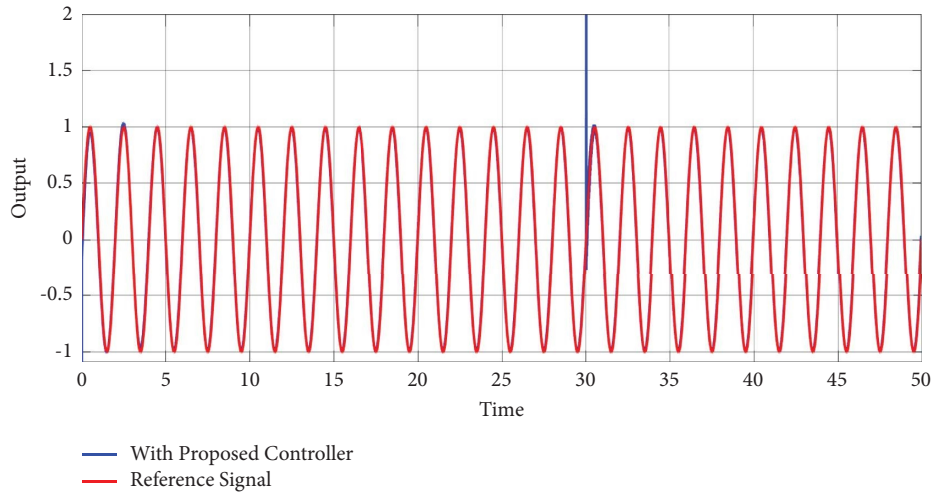

(a)

Figure 8: Continued.

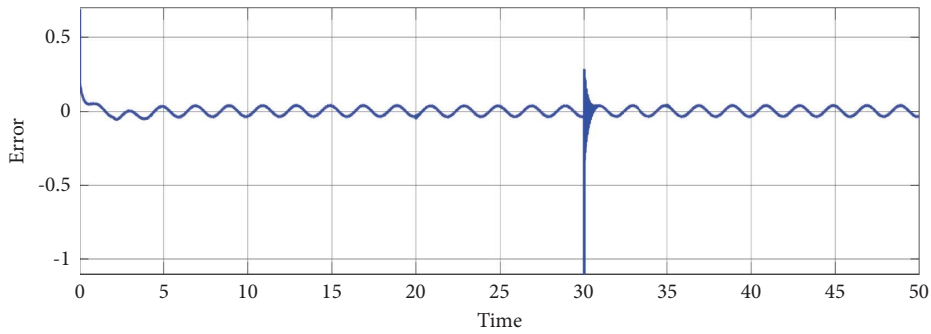

(b)

Figure 8: System output under output disturbance. (a) Output. (b) Error.

(MSE), the root mean square error (RMSE), and the standard deviation (S.D.). The following definitions can be assigned to these indices:

$$\begin{aligned} \text{MAE} &= \frac{1}{N}\sum_{k=1}^{N}|\varepsilon(k)|, \\ \text{S.D} &= \frac{1}{N}\sum_{k=1}^{N}(y(k)-\overline{y}), \\ \text{MSE} &= \frac{1}{N}\sum_{k=1}^{N}(\varepsilon(k))^2, \\ \text{RMSE} &= \sqrt{\frac{1}{N}\sum_{k=1}^{N}(\varepsilon(k))^2}. \end{aligned} \tag{58}$$

where the iterations number is defined as N and $\overline{y}$ is the output data mean value. Table 1 shows that the proposed controller's MAE, MSE, and RMSE indices have lower values than those of the other systems, i.e., [5, 25]. In light of this, it can be concluded that in the face of aperiodic and periodic disturbances as well as time-varying delay, the suggested controller improves system performance.

4.4. Case 4: Incorporating External Disturbances to the System's Output and Input Variables. The system's input and output are subjected to a disruption from outside in order to test the proposed scheme's robustness.

4.4.1. External Input Disturbance. The suggested controller is noticeably quick to adapt for the disturbance and provides good tracking performance by introducing an external input disturbance in the form of 30 amplitude step signal at time 30 s as depicted in the illustration of Figure 7.

4.4.2. External Output Disturbance. A perfect tracking performance may be obtained by applying an external step signal with an amplitude of 10 at a time for 30 s as illustrated in Figure 8 to the suggested controller, which corrects for external output disturbance. At the 30 s time, the projected controller effort is heightened to demonstrate the robustness of the APETM-MRC based on EID against external disturbances, as depicted in Figures 7 and 8.

5. Conclusions

This paper has looked at problems with tracking control and disturbance rejection for nonlinear systems with time-varying delays that are susceptible to undetected external disturbances. The suggested EID technique-based APETM-MRC has been created to provide disturbances' rejection, periodic reference tracking, and communication resource savings for the T-S fuzzy model. Both periodic and aperiodic disturbances are compensated using the EID-based MRC design. Additionally, the APETM has been implemented to transfer the data only when necessary in order to conserve communication resources and lower energy consumption. In order to respond to modifications in the system dynamics and save more computational resources, APETM has also researched an adaptive approach with a changing threshold. The LKF stability theorem has been used to formulate some suitable constraints in terms of LMIs in order to guarantee the stability of the closed-loop system. Due to the perfect optimal-solution accuracy and minimal computational complexity of the PSO, this technique is employed to look for the T-S based MRC system gains. The optimization of tuning parameters in a LKF is turned into the design of the MRC and controller parameters. The LMIs size increases in large-scale systems due to the larger number of parameters involved. As a result, the statistical efficiency diminishes, and difficulties arise in obtaining optimal gain values. To address this issue, a dimension reduction technique should be employed to enhance the statistical analysis in such cases. The simulation results of a physical model have been provided to guarantee the superiority and efficacy of the recommended strategy over competing schemes. Future areas of interest include expanding the proposed technique to be applicable to switched systems and networked control systems.

Additionally, there is a plan to combine the proposed controller with an adaptive fuzzy controller for some application.

Data Availability

No data were used to support the findings of this study.

Disclosure

Adnan Shakoor's present address is King Fahd University of Petroleum and Minerals, Dhahran 31261, Saudi Arabia.

Conflicts of Interest

The authors declare that they have no conflicts of interest.

Acknowledgments

The authors would like to acknowledge the support provided by the Deanship of Research Oversight and Coordination (DROC) at King Fahd University of Petroleum & Minerals (KFUPM) for funding this work through project no. EC231005.

References

[1] Y. R. Teo, A. J. Fleming, A. A. Eielsen, and J. Tommy Gravdahl, "A simplified method for discrete-time repetitive control using model-less finite impulse response filter inversion," *Journal of Dynamic Systems, Measurement, and Control*, vol. 138, no. 8, 2016.

[2] W. Sun, S.-F. Su, J. Xia, and Y. Wu, "Adaptive tracking control of wheeled inverted pendulums with periodic disturbances," *IEEE Transactions on Cybernetics*, vol. 50, no. 5, pp. 1867–1876, 2020.

[3] M. M. Gulzar, S. T. H. Rizvi, M. Y. Javed, U. Munir, and H. Asif, "Multi-agent cooperative control consensus: a comparative review," *Electronics*, vol. 7, no. 2, p. 22, 2018.

[4] Y. Liu, S. Cheng, B. Ning, and Y. Li, "Robust model predictive control with simplified repetitive control for electrical machine drives," *IEEE Transactions on Power Electronics*, vol. 34, no. 5, pp. 4524–4535, 2019.

[5] R. Sakthivel, P. Selvaraj, and B. Kaviarasan, "Modified repetitive control design for nonlinear systems with time delay based on T-S fuzzy model," *IEEE Transactions on Systems, Man, and Cybernetics*, vol. 50, no. 2, pp. 646–655, 2020.

[6] R. Sakthivel, K. Raajananthini, P. Selvaraj, and Y. Ren, "Design and analysis for uncertain repetitive control systems with unknown disturbances," *Journal of Dynamic Systems, Measurement, and Control*, vol. 140, no. 12, pp. 1–10, 2018.

[7] M. M. Gulzar, D. Sibtain, A. F. Murtaza, S. Murawwat, M. Saadi, and A. Jameel, "Adaptive fuzzy based optimized proportional-integral controller to mitigate the frequency oscillation of multi-area photovoltaic thermal system," *International Transactions on Electrical Energy Systems*, vol. 31, no. 1, Article ID e12643, 2021.

[8] G. Pipeleers, B. Demeulenaere, J. De Schutter, and J. Swevers, "Robust high-order repetitive control: optimal performance trade-offs," *Automatica*, vol. 44, no. 10, pp. 2628–2634, 2008.

[9] M. M. Gulzar, Q. Ling, M. Yaqoob, and S. Iqbal, "Realization of an improved path planning strategy," *International Conference on Control*, Automation and Information Sciences (ICCAIS), Changshu, China, 2015.

[10] C. Liu, X. Yue, J. Zhang, and K. Shi, "Active disturbance rejection control for delayed electromagnetic docking of spacecraft in elliptical orbits," *IEEE Transactions on Aerospace and Electronic Systems*, vol. 58, no. 3, pp. 2257–2268, 2022.

[11] R. Liu, G. Liu, M. Wu, J. She, and Z. Nie, "Robust disturbance rejection in modified repetitive control system," *Systems & Control Letters*, vol. 70, pp. 100–108, 2014.

[12] L. Zhou, J. She, X. M. Zhang, and Z. Zhang, "Improving disturbance-rejection performance in a modified repetitive-control system based on equivalent-input-disturbance approach," *International Journal of Systems Science*, vol. 51, no. 1, pp. 49–60, 2020.

[13] Y. Wu and J. Dong, "Local stabilization of continuous-time T–S fuzzy systems with partly measurable premise variables and time-varying delay," *IEEE Transactions on Systems, Man, and Cybernetics*, vol. 51, no. 1, pp. 326–338, 2021.

[14] M. Hamdy, R. Shalaby, and M. Sallam, "Experimental verification of a hybrid control scheme with chaotic whale optimization algorithm for nonlinear gantry crane a comparative study," *ISA Transactions*, vol. 98, pp. 418–433, 2020.

[15] Y. Lei, Y.-W. Wang, Z.-H. Guan, and Y.-J. Shen, "Event-triggered adaptive output regulation for a class of nonlinear systems with unknown control direction," *IEEE Transactions on Systems, Man, and Cybernetics*, vol. 50, no. 9, pp. 3181–3188, 2020.

[16] D. Sibtain, M. M. Gulzar, K. Shahid, I. Javed, S. Murawwat, and M. M. Hussain, "Stability analysis and design of variable step-size P&O algorithm based on fuzzy robust tracking of MPPT for standalone/grid connected power system," *Sustainability*, vol. 14, no. 15, p. 8986, 2022.

[17] Y. Wang, L. Zheng, H. Zhang, and W. Zheng, "Fuzzy observer-based repetitive tracking control for nonlinear systems," *IEEE Transactions on Fuzzy Systems*, vol. 28, no. 10, pp. 2401–2415, 2020.

[18] M. Zhang, M. Wu, L. Chen, S. Tian, and J. She, "Optimisation of control and learning actions for a repetitive-control system based on Takagi–Sugeno fuzzy model," *International Journal of Systems Science*, vol. 51, no. 15, pp. 3030–3043, 2020.

[19] S. Abd-Elhaleem, M. Soliman, and M. Hamdy, "Periodic event-triggered modified repetitive control with equivalent-input-disturbance estimator based on T-S fuzzy model for nonlinear systems," *Soft Computing*, vol. 26, no. 13, pp. 6443–6459, 2022.

[20] S. Abd-Elhaleem, M. Soliman, and M. Hamdy, "Modified repetitive periodic event-triggered control with equivalent-input-disturbance for linear systems subject to unknown disturbance," *International Journal of Control*, vol. 95, no. 7, pp. 1825–1837, 2022.

[21] P. Mani, R. Rajan, and Y. H. Joo, "Design of observer-based event-triggered fuzzy ISMC for T—S fuzzy model and its application to PMSG," *IEEE Transactions on Systems, Man, and Cybernetics*, vol. 51, no. 4, pp. 2221–2231, 2021.

[22] Z. Gu, D. Yue, and E. Tian, "On designing of an adaptive event-triggered communication scheme for nonlinear networked interconnected control systems," *Information Sciences*, vol. 422, pp. 257–270, 2018.

[23] L. Zhang, H. Liang, Y. Sun, and C. K. Ahn, "Adaptive event-triggered fault detection scheme for semi-markovian jump systems with output quantization," *IEEE Transactions on Systems, Man, and Cybernetics*, vol. 51, no. 4, pp. 2370–2381, 2021.

[24] C. Liu, X. Yue, K. Shi, and Z. Sun, *Spacecraft Attitude Control: A Linear Matrix Inequality Approach*, Elsevier, Amsterdam, The Netherlands, 2022.

[25] P. Selvaraj, R. Sakthivel, and H. R. Karimi, "Equivalent–input–disturbance based repetitive tracking control for Takagi—sugeno fuzzy systems with saturating actuator," *IET Control Theory & Applications*, vol. 10, no. 15, pp. 1916–1927, 2016.